Redox Biology 21 (2019) 101120

Contents lists available at ScienceDirect

Redox Biology

journal homepage: www.elsevier.com/locate/redox

Mst1 inhibition attenuates non-alcoholic fatty liver disease via reversing Parkin-related mitophagy

Tao Zhou[a,1], Ling Chang[b,1], Yi Luo[a,1], Ying Zhou[b,*], Jianjun Zhang[a,**]

[a] Department of Liver Surgery, Renji Hospital, School of Medicine, Shanghai Jiao Tong University, Shanghai, China
[b] Department of Gastroenterology, The Seventh People's Hospital of Shanghai University of Traditional Chinese Medicine, Shanghai, China

ARTICLE INFO

Keywords:
Non-alcoholic fatty liver disease
Parkin-related mitophagy
Mitochondrial damage
Mst1

ABSTRACT

Obesity-related non-alcoholic fatty liver disease (NAFLD) is connected with mitochondrial stress and hepatocyte apoptosis. Parkin-related mitophagy sustains mitochondrial homeostasis and hepatocyte viability. However, the contribution and regulatory mechanisms of Parkin-related mitophagy in NAFLD are incompletely understood. Macrophage stimulating 1 (Mst1) is a novel mitophagy upstream regulator which excerbates heart and cancer apoptosisn via repressing mitophagy activity. The aim of our study is to explore whether Mst1 contributes to NAFLD via disrupting Parkin-related mitophagy. A NAFLD model was generated in wild-type (WT) mice and Mst1 knockout (Mst1-KO) mice using high-fat diet (HFD). Cell experiments were conducted via palmitic acid (PA) treatment in the primary hepatocytes. The results in our study demonstrated that Mst1 was significantly upregulated in HFD-treated livers. Genetic ablation of Mst1 attenuated HFD-mediated hepatic injury and sustained hepatocyte viability. Functional studies illustrated that Mst1 knockdown reversed Parkin-related mitophagy and the latter protected mitochondria and hepatocytes against HFD challenge. Besides, we further figured out that Mst1 modulated Parkin expression via the AMPK pathway; blockade of AMPK repressed Parkin-related mitophagy and recalled hepatocytes mitochondrial apoptosis. Altogether, our data identified that NAFLD was closely associated with the defective Parkin-related mitophagy due to Mst1 upregulation. This finding may pave the road to new therapeutic modalities for the treatment of fatty liver disease.

1. Introduction

It is considered an emerging health problem due to high-fat diet (HFD) intake. Nonalcoholic fatty liver disease (NAFLD) occurs due to excessive fat deposition in hepatocyte. The consequential surplus of lipids in hepatocytes results in oxidative stress and lipotoxicity, and it promotes mitochondrial dysfunction via multiple mechanisms [1,2]. Mitochondrial damage triggers hepatocyte death or dysfunction, which is one of the most important features of NAFLD [3]. With the loss of functional liver tissue, hepatic stellate cells are activated and contribute to the accumulation of extracellular matrix proteins, leading to fibrosis. Thus, protecting mitochondria against lipotoxicity is vital to retard or reverse the progression of NAFLD.

In response to mitochondrial damage, mitochondria could repair itself with the assistance of lysosome [4,5]. This process is termed as mitochondrial autophagy or mitophagy. Several studies have reported the beneficial roles played by mitophagy in regulating acute and chronic hepatic injury. For example, Bnip3-mediated mitophagy sustains mitochondrial function and favors hepatocyte survival in fatty liver disease [2]. FUNDC1-related mitophagy suppresses hepatocarcinogenesis via inhibition of inflammasome activation [6,7]. During liver ischemia-reperfusion injury, ROS-modified mitophagy regulates liver endothelial cell apoptosis [8]. In NAFLD, mitophagy is significantly inhibited and defective mitophagy is deemed as the pathogenesis for the development of fatty liver disease [9]. Many researchers have attempted to illustrate the protective effects exerted by mitophagy in NAFLD. However, there have been no studies investigating the upstream regulatory mechanism for mitophagy inhibition under chronic high-fat stress.

Macrophage stimulating 1 (Mst1), a novel regulator of cell survival, has been found to be associated with liver regeneration. Genetic ablation of Mst1 promotes liver repair and regeneration in aged mice [10]. Besides, Mst1 disrupts hepatic lipid metabolism via suppressing Sirt1

* Correspondence to: Department of Gastroenterology, The Seventh People's Hospital of Shanghai University of Traditional Chinese Medicine, 358 Datong Road, Shanghai 200137, China.
** Correspondence to: Department of Liver Surgery, Renji Hospital, School of Medicine, Shanghai Jiao Tong University, 160 Pujian Road, Shanghai 200127, China.
E-mail addresses: drzhouying@126.com (Y. Zhou), dr_rjzhangjianjun@126.com (J. Zhang).
[1] These authors shared co-first authorship.

https://doi.org/10.1016/j.redox.2019.101120
Received 31 December 2018; Received in revised form 16 January 2019; Accepted 22 January 2019
Available online 23 January 2019

ubiquitination [11]. In addition, Mst1 inhibition ameliorates hepatic steatosis in a manner dependent on IRS2/Akt signaling [12]. These results indicate that Mst1 may be connected to liver metabolic disorder. With respect to mitophagy, Mst1 has been well recognized as major inhibitor controlling mitophagy activation. In cardiac ischemia-reperfusion injury, Mst1 inactivates FUNDC1-related mitophagy via downregulating the ERK-CREB pathways [13,14]. Besides, Mst1 also promotes endometriosis progression via suppressing Parkin-required mitophagy [15]. In colorectal cancer, Mst1 inhibits Bnip3-related mitophagy via the JNK/p53 pathways [16]. Such evidence potentially implies that Mst1 may have the ability to suppress mitophagy during fatty liver disease. However, this remains to be elucidated. Accordingly, the aim of our study was to explore the role of Mst1 in fatty liver disease and figure out whether Mst1 affects the NAFLD via inactivating Parkin-related mitophagy.

2. Materials and methods

2.1. Ethical statement

Experimental protocol was approved by Shanghai Jiao Tong University, School of Medicine. All animal researches were carried out according to the guidelines of Animal Care and Use Committee of Renji Hospital, School of Medicine, Shanghai Jiao Tong University, Shanghai, China. All efforts were done to minimize suffering of experimental rats in this research.

2.2. Animal treatment

Sixty male wild-type (WT) mice and Mst1 knockout (Mst1-KO) mice were obtained from University of Science and Technology (K&D gene technology, WuHan, China) according to a previous study [17]. These mice (six-week-old) were firstly housed for two weeks of acclimation in a temperature controlled room under 12/12 h light/dark cycle and had free access to food and water. To induce the NAFLD, the above mice were continuously fed either a high-fat diet (HFD) or a normal chow (low-fat diet (LFD)) diet for 12 weeks based on a previous study [1].

2.3. Biochemical evaluation

Levels of alanine transaminase (ALT), aspartate transaminase (AST), triglyceride, total cholesterol, leptin, and adiponectin, in serum were determined to evaluate liver injury using a HITACHI 7020 automatic biochemical analyzer (Hitachi, Tokyo, Japan) and commercial reagent kit (Kehua Bio-engineering, Shanghai, China) [18,19].

2.4. Liver histology

For histological analyses, liver tissues were embedded in 4% buffered formalin, and then, 5 μm tissue sections were prepared. Subsequently, the sections were stained with HE (hematoxylin and eosin) and Sirius Red. An Olympus light microscope (Olympus, Tokyo, Japan) was used to observe the samples. The histologic changes after tubular injury were evaluated semi-quantitatively according to a previous study [20].

2.5. Primary hepatocytes culture

Primary hepatocytes from WT mice and Mst1-KO mice (8–9 weeks) were isolated and cultured according to the method described previously. The primary hepatocytes were cultured in Dulbecco's modified Eagle's medium supplemented with 10% Fetal Bovine serum, 2 mM glutamine, 1% penicillin/streptomycin solution (all reagents from Sigma-Aldrich, St Louis, MO) at 37 °C in 5% CO_2. Palmitic acid (PA, 75 μmol/L; Sigma-Aldrich) was used to incubate with primary hepatocytes for 24 h to mimic the high-fat stress *in vitro*. To inhibit the AMPK pathway, Compound C (CC, Selleck Chemicals, Houston, TX, USA) were administrated into the medium of cell for 2 h [21].

2.6. Confocal microscopy

For confocal analysis, the cells were fixed with 4% paraformaldehyde for 30 min at room temperature. After a 10-min incubation with 3% hydrogen peroxide to block endogenous peroxidase activity, the samples were incubated with primary antibodies overnight at 4 °C. Then, the slides were washed with PBS and incubated with a secondary antibody (1:500, Invitrogen, Carlsbad, CA, USA) at room temperature for 45 min [22]. The nuclei were stained using DAPI. The images were acquired via fluorescence microscopy (Olympus BX-61). The following primary antibodies were used in the present study: p-AMPK (1:1000, Abcam, #ab23875), Tom20 (1:1000, Abcam, #ab186735), LAMP1 (1:1000, Abcam, #ab24170), cleaved caspase3 (1:1000, Abcam, #ab49822), caspase9 (1:1000, Cell Signaling Technology, #9504), Parkin (1:1000, Cell Signaling Technology, Inc.) [23].

2.7. Western blot analysis

Each group of samples was collected, the cell lysates were prepared, and the total protein was extracted and quantified using a BCA protein concentration kit according to the manufacturer's instructions [24]. The proteins were separated by sodium dodecyl sulfate polyacrylamide gel electrophoresis and transferred to polyvinylidene fluoride membranes. The membranes were blocked with 5% BSA in Tris-buffered saline with Tween-20 (TBST) for 2 h at room temperature and incubated with primary antibodies overnight at 4 °C. The membranes were washed three times with PBS; IRDye 800CW goat anti-rabbit IgG (H + L) (926–32211; Licor, Lincoln, NB, USA) was added; and the membranes were incubated at 37 °C for 1 h [25]. The bands were detected using a chemiluminescent imaging system. The primary antibodies used in the present study were as follows: Parkin (1:1000, Cell Signaling Technology, Inc. #2132), Bcl2 (1:1000, Cell Signaling Technology, #3498), Bax (1:1000, Cell Signaling Technology, #2772), caspase9 (1:1000, Cell Signaling Technology, #9504), pro-caspase3 (1:1000, Abcam, #ab13847), cleaved caspase3 (1:1000, Abcam, #ab49822), c-IAP (1:1000, Cell Signaling Technology, #4952), survivin (1:1000, Cell Signaling Technology, #2808), Bad (:1000; Abcam; #ab90435), cyt-c (1:1000; Abcam; #ab90529), LC3II (1:1000, Cell Signaling Technology, #3868), Vps34 (1:1000, Cell Signaling Technology, #4263), Tim23 (1:1000, Santa Cruz Biotechnology, #sc-13298), Tom20 (1:1000, Abcam, #ab186735), AMPK (1:1000, Abcam, #ab131512), p-AMPK (1:1000, Abcam, #ab23875). The secondary antibodies used in the present study were: Horseradish peroxidase (HRP)-coupled secondary antibodies (1:2000; cat. nos. 7074 and 7076; Cell Signaling Technology, Inc.). Band intensities were normalized to the respective internal standard signal intensity (GAPDH (1:1000, Cell Signaling Technology, #5174) and/or β-actin (1:1000, Cell Signaling Technology, #4970) using Quantity One Software (version 4.6.2; Bio-Rad Laboratories, Inc.).

2.8. Oxidative stress detection

Liver oxidative stress were measured via ELISA. The concentration of MDA, SOD, GSH-PX were determined using the commercial kits (Nanjin Jiancheng Bioengineering Institute, Nanjing, China) according to the manufacturer's instructions [26,27]. The cellular oxidative markers were also determined via ELISA according to the previous study. The concentration of antioxidant such as SOD, GSH and GPX were measured based on the instructions of the manufacturer (Beyotime, China). The results are expressed as nmol/g tissue.

2.9. Cell viability detection

Cell death was measured via a TUNEL assay using an in situ cell death detection kit (Roche, Indianapolis, IN, USA). The TUNEL kit was

used to stain nuclei containing fragmented DNA [28]. Cells were fixed with 3.7% paraformaldehyde for 30 min at room temperature. Subsequently, the samples were incubated with equilibration buffer, nucleotide mix and rTdT enzyme at 37 °C for 60 min. Then, a saline-sodium citrate buffer was used to stop the reaction. After being loaded with DAPI, the samples were visualized via fluorescence microscopy (Olympus BX-61). In addition, an MTT assay was performed to analyse the cell viability according to methods described in a previous study [29,30]. Absorbance was determined at 570 nm. The relative cell viability was recorded as a ratio to that in the control group.

2.10. Mitochondrial function analysis

Mitochondrial membrane potential was observed via JC-1 staining according to the previous study [31]. mPTP opening was evaluated based on a previous study using calcein-AM/cobalt. The relative mPTP opening rate was recorded as the ratio to control group [32]. ATP production was measured using Enhanced ATP Assay Kit (Beyotime, China, Cat. No: S0027). Flow cytometry was used to analyse mitochondrial ROS (mROS) production. Cells were washed three times with PBS and then resuspended in PBS using 0.25% trypsin. Subsequently, the cells were incubated with the MitoSOX red mitochondrial superoxide indicator (Molecular Probes, USA) for 15 min at 37 °C in the dark [33]. After three washes with PBS, mROS production was analyzed via flow cytometry (Sysmex Partec GmbH, Görlitz, Germany), and the data were analyzed using Flowmax software (Sysmex Partec, Version 2.3, Germany) [34].

2.11. RNA interference

In the present study, 4×10^5 cells/well were transfected with 100 pmol siRNA in 6 well plates by Lipofectamine RNAiMAX (Invitrogen) as indicated by the supplier. Transfection was performed overnight and two independent siRNAs against Parkin were transfected into cell with the help of FuGENE transfection reagent (E2312, Roche, Indianapolis, IN, USA). The knockdown efficiency was determined via western blotting [35,36].

2.12. Statistical analyses

All statistical analyses were conducted with the Prism graphical software (GraphPad, Software). Data were generated from multiple repeats of different biological experiments to obtain the mean values and s.e.m displayed throughout. Statistical differences were measured using one-way ANOVA with Bonferroni or Dunnett corrections for multiple comparisons when appropriate. Significance was set at $P < 0.05$.

3. Results

3.1. Mst1 deletion prevents diet-induced NAFLD

Firstly, Mst1 expression was analyzed using qPCR and western blotting. Compared to the low-fat diet (LFD)-treated mice, Mst1 was abundant in high-fat fed (HFD)-treated liver at both the transcription (Fig. 1A) and expression levels (Fig. 1B-C). This finding was further supported *in vitro* using the primary hepatocytes and PA-mediated lipotoxicity model. Compared to the control group, Mst1 expression was obviously upregulated via western blotting (Fig. 1D-E). This information indicated that high-fat stress caused Mst1 activation in liver tissue. Subsequently, to observe the functional role of Mst1 in fatty liver disease, Mst1 knockout (Mst1-KO) mice were used. Then, the biological characterization of Mst1-KO mice in the presence of high-fat stress was monitored. Body weight, fasting blood glucose, and metabolism parameters were measured. HFD-treated mice exhibited increased body weight (Fig. 1F) and higher levels of blood glucose (Fig. 1G). Not surprisingly, Mst1 deletion reduced body weight (Fig. 1F) and repressed the levels of blood glucose (Fig. 1G). Moreover, the concentration of triglycerides, total cholesterol, aspartate transaminase (AST) and alanine transaminase (ALT) levels, were all elevated in HFD mice but reduced in the Mst1-deleted mice (Fig. 1H-K). Altogether, these data illustrated that chronic high-fat stress caused Mst1 upregulation, and Mst1 deletion reduced the HFD-induced hepatic injury.

3.2. Mst1 deletion improves liver function

Next, liver structure was observed in response to Mst1 deletion. First, the liver weight was significantly increased in HFD-treated mice (Fig. 2A), indicative of hepatic sclerosis. However, this effect was negated by Mst1 deletion. Subsequently, HE staining and Sirius Red staining were performed to observe the hepatocyte vacuolation, steatosis, and fibrosis, respectively. As shown in Fig. 2B, HFD treatment increased the average diameter of hepatocyte, and this effect could be reversed by Mst1 deletion. In addition, chronic HFD stress promoted liver fibrosis, and this phenotypic alteration could be negated by Mst1 deletion (Fig. 2C). At the molecular levels, the lipogenic genes such as PPARα, ACCA1, SREBP1c, and FAS1 were significantly increased in response to HFD treatment (Fig. 2D-G), and these parameters were suppressed by Mst1 deletion. In addition, the signaling pathways related to liver fibrosis, such as TGFβ and MMP9 were obviously activated by HFD and were inhibited by Mst1 ablation (Fig. 2H-J). Altogether, these data indicated that Mst1 deletion reduced HFD-mediated hepatic injury.

3.3. Mst1 deletion attenuates HFD-mediated liver oxidative stress and the inflammation response

Oxidative stress and the inflammation response are thought to be the primary reasons for high-fat-mediated liver function deterioration. Based on this information, experiments were performed to analyse the alteration of oxidative stress markers and the inflammation reaction. First, liver antioxidant factors such as SOD and GSH-PX were downregulated in HFD-treated mice and were reversed to near-normal levels in Mst1-KO mice (Fig. 3A-B). By comparison, oxidative products such as GSSG (oxidized form of GSH) and MDA were increased in HFD-treated livers and were reduced in livers with Mst1 deletion (Fig. 3C-D). Altogether, this information indicated that Mst1 deletion sustained the antioxidant activity of livers in answer to HFD stress.

With respect to inflammation, ELISA assays demonstrated that the serum TNFα, IL-6 and MCP1 were all increased in the HFD-treated mice, and this tendency was reversed by Mst1 deletion (Fig. 3E-G). Moreover, western blotting using liver tissues illustrated that TNFα, IL-8 and MIP1α were markedly elevated in response to HFD treatment and were reduced to near-normal levels with Mst1 deletion (Fig. H-K). Altogether, these findings supported the functional importance of Mst1 in agitating high-fat-evoked oxidative stress and the inflammation response.

3.4. Mst1 knockdown attenuates hepatocyte mitochondrial apoptosis

Mitochondrial damage has been reported to be the potential target of lipotoxicity. Accordingly, next experiments were performed to observe high-fat-mediated hepatocyte mitochondrial apoptosis. *In vivo*, immunofluorescence assays using the cleaved caspase-3 and caspase-9 antibodies demonstrated that HFD treatment increased the fluorescence intensity of caspase-3/9 in liver tissues(Fig. 4A-B), and this effect was reversed by Mst1 knockdown. This finding was further supported by western blotting. As shown in Fig. 4C-F, HFD treatment elevated the expression of mitochondrial pro-apoptotic proteins such as caspase-3 and caspase-9. In contrast, the expression of mitochondrial anti-apoptotic factors such as c-IAP was downregulated, ccorrespondingly. Interestingly, Mst1 knockdown could repress the pro-apoptotic protein upregulation and reverse the content of anti-apoptotic factors (Fig. 4C-F).

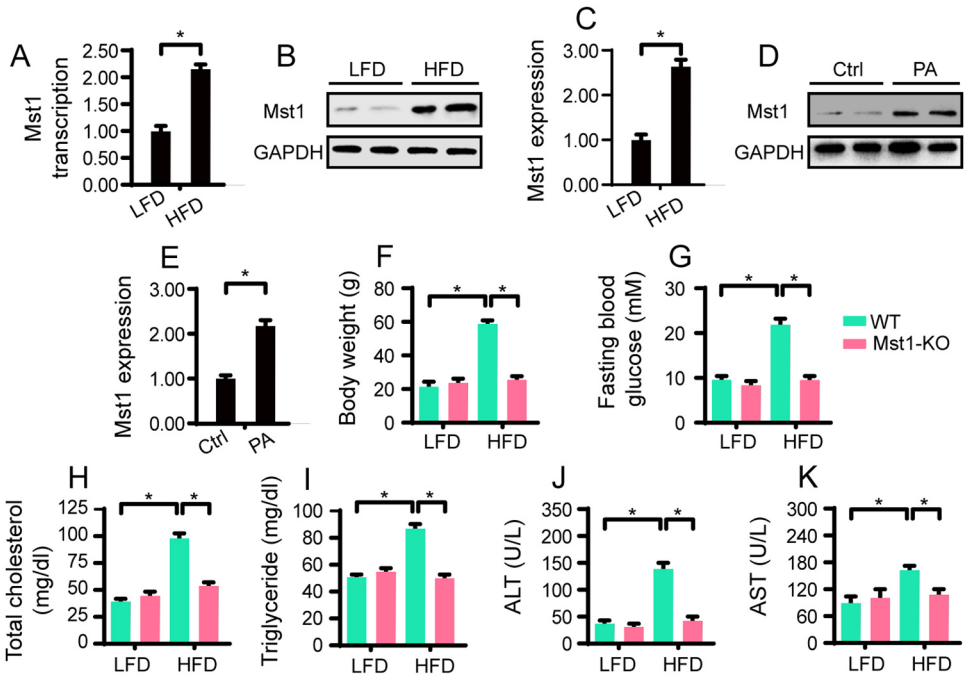

Fig. 1. Mst1 is upregulated in HFD-treated liver tissues and contributes to the development of NAFLD. A. The transcription levels of Mst1 in livers from low-fat diet (LFD)-treated mice or high-fat diet (HFD)-treated mice. B-C. The protein expression of Mst1 in livers from LFD-treated mice or HFD-treated mice. D-E. *In vitro,* primary hepatocytes were treated with PA. The protein expression of Mst1 was determined via western blotting. F. Body weight was measured to explore the role of Mst1 in body weight gain. G. Blood glucose levels were measured in WT mice and Mst1-KO mice. H-K. The levels of triglyceride, total cholesterol, ALT and AST in the blood isolated from WT mice and Mst1-KO mice using ELISA. Experiments were repeated three times, and data are shown as the means ± SEM. n = 6 mice per group. $^*P < 0.05$.

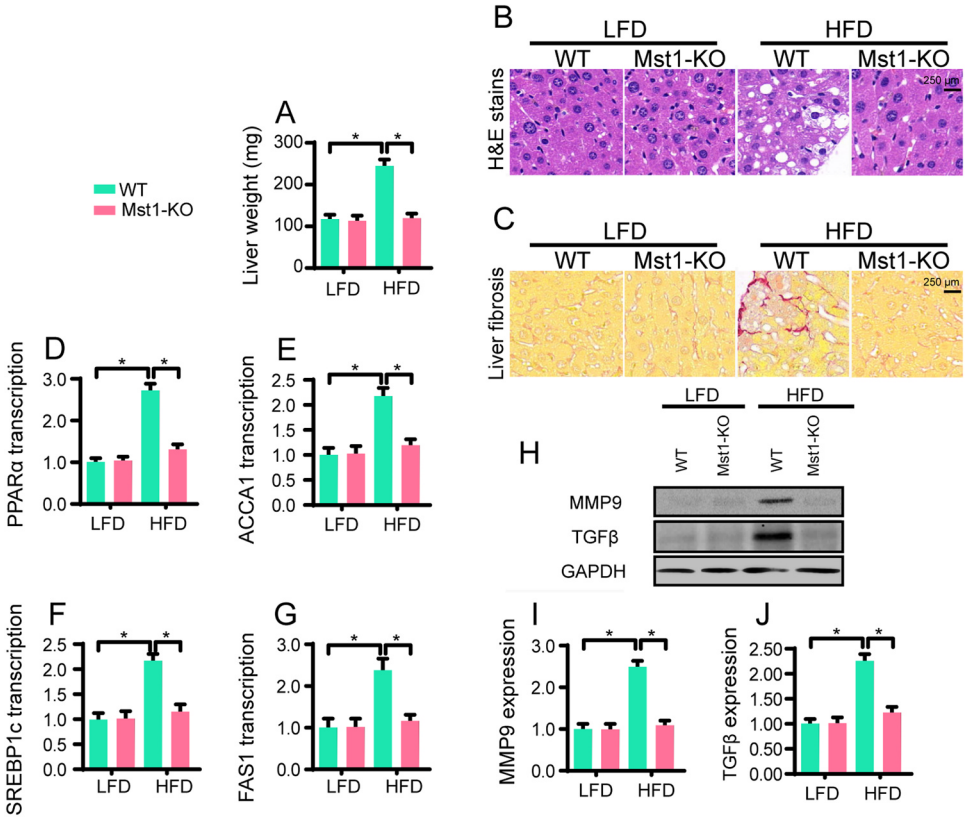

Fig. 2. Genetic ablation of Mst1 attenuates liver injury in HFD-treated mice. A. The liver weight was measured in WT mice and Mst1-KO mice. B. The livers were obtained and the HE staining was performed to observe the structural alterations in HFD-treated livers with Mst1 knockdown. C. Sirius red staining for livers isolated from WT mice and Mst1-KO mice. The red area means the renal fibrosis. D-G. qPCR assay was used to analyse the alterations of lipogenic genes such as PPARα, ACCA1, SREBP1c, and FAS1. H-J. Proteins were isolated from livers tissues in WT mice and Mst1-KO mice. Then, western blotting was performed to observe the changes in fibrosis-related signaling pathways. Experiments were repeated three times, and data are shown as the means ± SEM. n = 6 mice per group. $^*P < 0.05$.

In vitro, the primary hepatocytes were cultured with PA and then Mst1 knockdown assay was achieved using Mst1 siRNA. Subsequently, the apoptotic index was evaluated via TUNEL assay. As shown in Fig. 4G-H, the number of TUNEL-positive cells was drastically increased in response to PA stress. Interestingly, Mst1 siRNA strongly repressed PA-induced cell apoptosis (Fig. 4G-H). This finding was further validated via analyzing the cellular viability using MTT assay. As shown in Fig. 4I, the PA-initiated cell viability was reversed by Mst1 knockdown. Altogether, these data suggested that Mst1 ablation alleviated mitochondrial apoptosis in high-fat-treated livers *in vitro* and *in vivo.*

3.5. Mst1 knockdown increases Parkin expression and thus reverses mitophagy activity

In response to mitochondrial damage, mitochondria would repair itself with the help of lysosome, and this process is identified as mitophagy [37]. In the present study, we explored whether Mst1 knockdown attenuated mitochondrial injury via activating mitophagy.

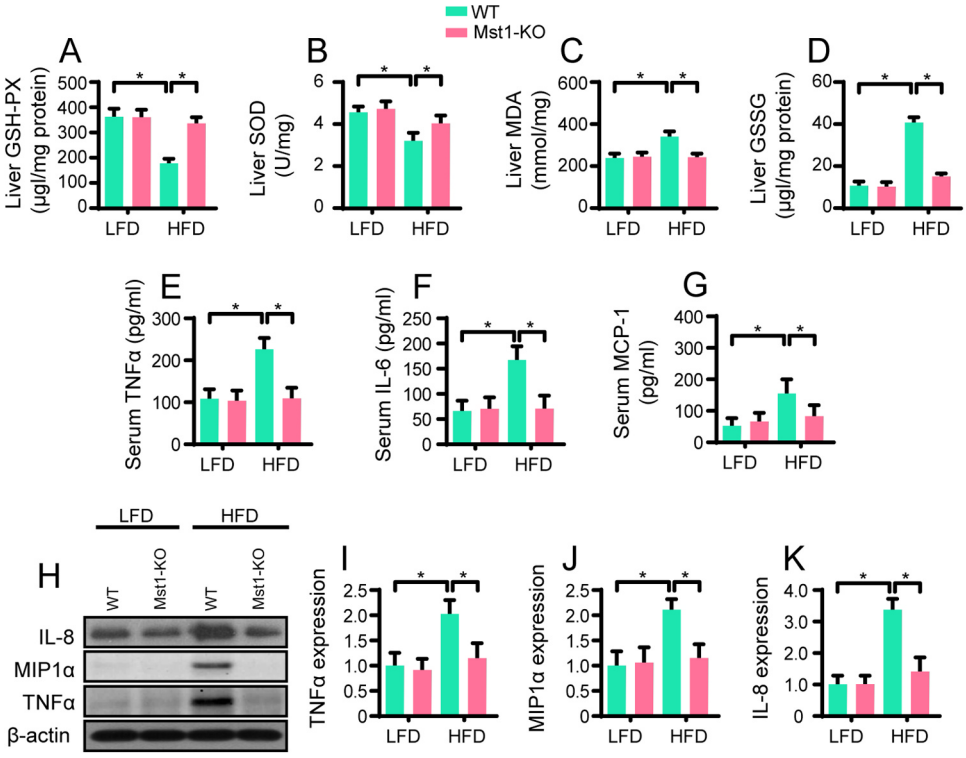

Fig. 3. Mst1 knockdown represses HFD-mediated liver oxidative stress and the inflammation response. A-D. Livers were collected and the proteins were isolated to analyse the oxidative stress markers via ELISA assay. E-G. Blood was collected from WT mice and Mst1-KO mice; then, serum TNFα, IL-6, and MCP-1 were measured via ELISA assay. H-K. Western blotting was performed to analyse the protein expression of inflammation factors. Experiments were repeated three times and data are shown as the means ± SEM. n = 6 mice per group. $^*P < 0.05$.

Firstly, mitophagy-related factors were detected via western blotting and these parameters were chosen based on the previous reports [4,38]. Compared to the control group, the ratio of LC3II/LC3I was significantly reduced in response to PA treatment, indicative of an autophagosome synthesis defect (Fig. 5A-B). Subsequently, mitochondria were isolated and the expression of mitochondrial LC3II (mito-LC3II) was analyzed. Similarly, the level of mito-LC3II was obviously down-regulated in PA-treated hepatocytes (Fig. 5C), an effect that was accompanied with an increase in Tom-20 and Tim-23 (mitochondrial outer and inner membrane markers) (Fig. 5A-F). Besides, the expression

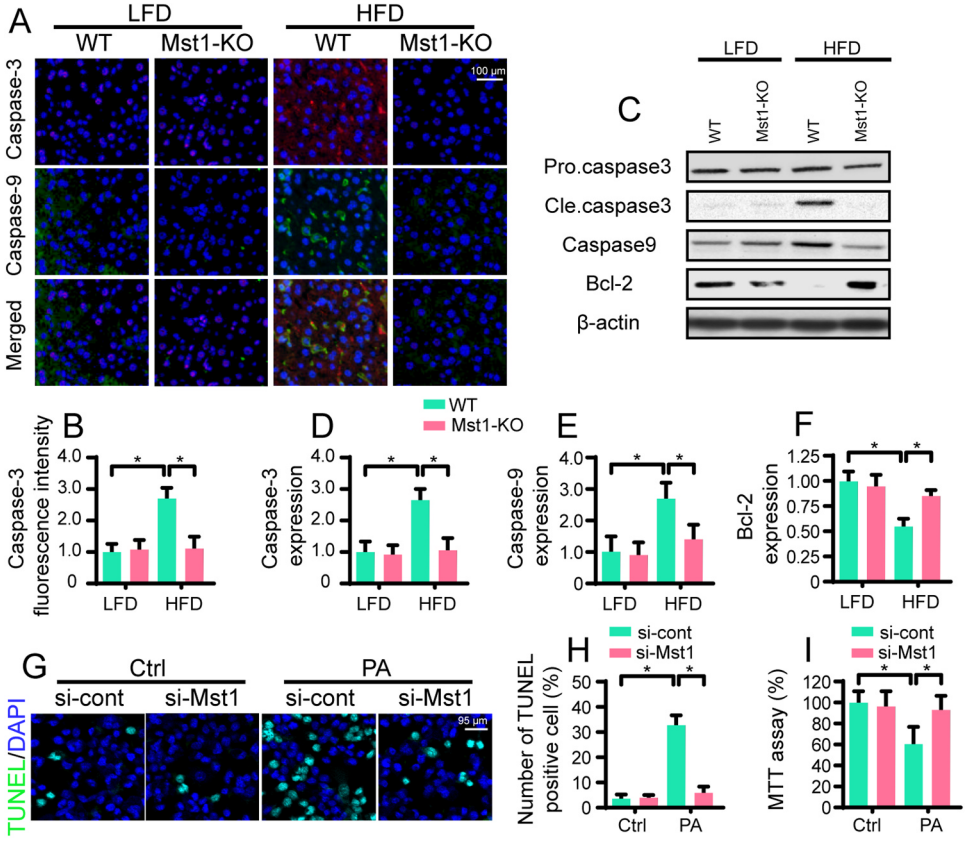

Fig. 4. Mst1 inhibition reduces PA-induced hepatocyte mitochondrial apoptosis. A-B. Immunofluorescence assay for caspase-3 and caspase-9 *in vivo*. The fluorescence intensity of caspase-3 and caspase-9 were significantly increased in response to chronic HFD treatment and was reduced by Mst1 knockdown. C-F. Proteins were isolated in WT mice and Mst1-KO mice; then, western blotting was performed to analyse the apoptotic protein expression. G-H. *In vitro*, primary hepatocytes were treated with PA and then, TUNEL staining was used to quantify the apoptotic cell. To repress the Mst1 expression, siRNA-against Mst1 (si-Mst1) was transfected into cells before PA stimulus. I. Hepatocyte viability was measured via MTT assay. Experiments were repeated three times and data are shown as the means ± SEM. n = 6 mice per group. $^*P < 0.05$.

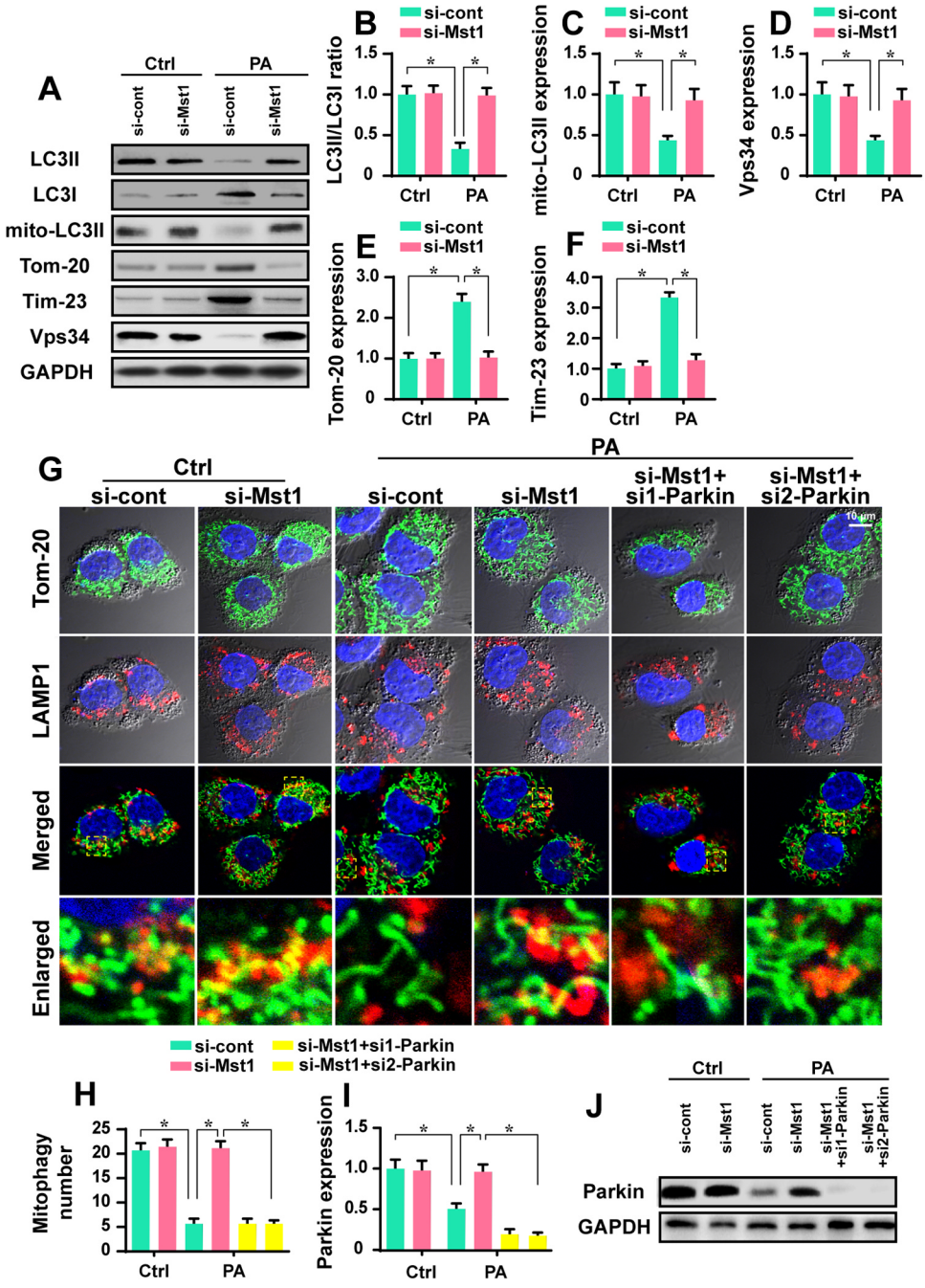

Fig. 5. Mst1 inactivates the mitophagy activity via repressing Parkin expression. A-F. *In vitro*, primary hepatocytes were treated with PA. Proteins were isolated from cells and western blotting was used to observe the alterations of mitophagy-related factors. G-H. Immunofluorescence assay for mitophagy. Tom-20 and LAMP1 were used to label mitochondria and lysosome, respectively. Then, the number of mitophagy was recorded. I-J. Western blotting was used to detect the expression of Parkin in response to Mst1 knockdown. Two independent Parkin siRNA (si1-Parkin and si2-Parkin) were used to inhibit Parkin expression. The knockdown efficiency was verified via western blotting. Experiments were repeated three times and data are shown as the means ± SEM. n = 6 mice per group. $^{*}P < 0.05$.

of Vps34 was obviously reduced by PA treatment compared to that in control group (Fig. 5A-F). These information indicated that mitophagy was largely inhibited by PA in hepatocyte. Interestingly, loss of Mst1 reversed the mitophag activity in the presence of PA stress, as evidenced by augmented LC3II/LC3I ratio, increased mito-LC3II expression and decreased Tom-20/Tim-23 levels (Fig. 5A-F).

To further observe the mitophagy activity, immunofluorescence assay was performed using mitochondria and lysosome antibodies. Under physiological conditions, green mitochondria communicated with red lysosome generating orange mitophagy (Fig. 5G-H). Interestingly, the number of orange dots was significantly reduced by PA treatment, indicative of mitophagy inhibition (Fig. 5G-H). However, Mst1 knockdown promoted the cooperation between mitochondria and lysosome and thus reversed the number of mitophagy. These data underscored the inhibitory effects of Mst1 on mitophagy in PA-treated hepatocytes.

Parkin has been found to be the primary factor for mitophagy activation. Accordingly, we asked whether Mst1 knockdown reversed mitophagy activity via upregulating Parkin expression. As shown in Fig. 5I-J, compared to the control group, PA treatment reduced the expression of Parkin, and this effect was abolished by Mst1. To further explain whether Parkin was required for Mst1-modulated mitophagy, two independent siRNAs were transfected into the Mst1-deleted cells to prevent Parkin upregulation. The knockdown efficiency was confirmed via western blotting (Fig. 5I-J). Then, Mst1-modified mitophagy was evaluated using immunofluorescence. Compared to the Mst1-deleted cells, knockdown of Parkin disrupted the fusion between mitochondria and lysosome, an effect that was accompanied with a drop in the number of mitophagy (Fig. 5G-H). Altogether, our results indicated that mitophagy was largely inactivated by Mst1 via reducing Parkin expression in the presence of high-fat stress.

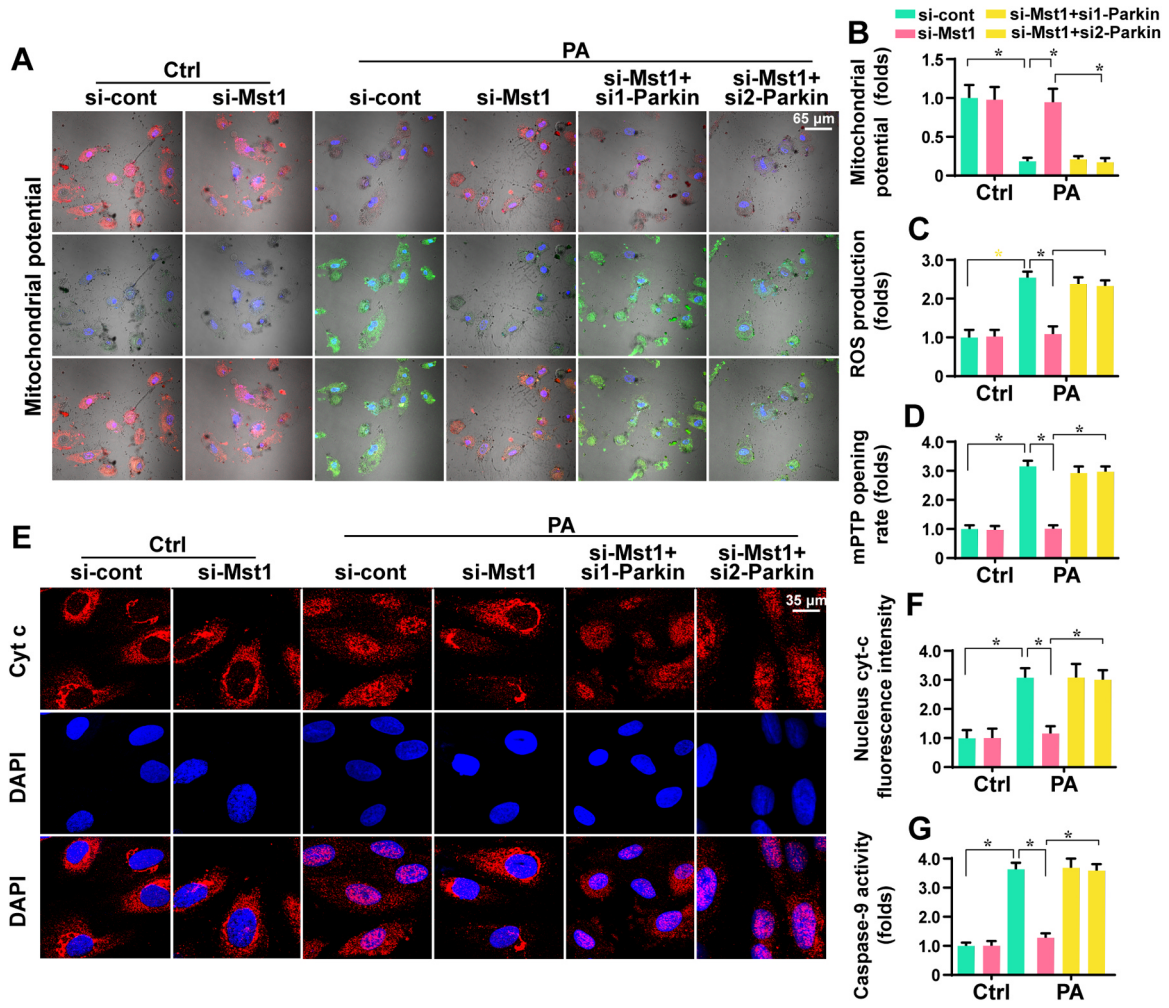

Fig. 6. Parkin-related mitophagy sustains mitochondrial homeostasis. A-B. *In vitro*, primary hepatocytes were treated with PA and then, JC-1 probe was used to observe mitochondrial potential. Two independent Parkin siRNA (si1-Parkin and si2-Parkin) were used to inhibit Parkin expression. C. Mitochondrial ROS (mROS) was analyzed using flow cytometry. siRNA against Parkin was used to inhibit Parkin expression. D. mPTP opening rate was detected and PA-mediated mPTP opening could be repressed by Mst1 knockdown in a manner dependent on Parkin-related mitophagy. E-F. Immunofluorescence assay for cyt-c staining. DAPI was used to label nucleus. G. Mitochondrial apoptosis was measured via detecting caspase-9 activity. Experiments were repeated three times and data are shown as the means ± SEM. n = 6 mice per group. $^{*}P < 0.05$.

3.6. Loss of Parkin-related mitophagy abrogates the protective effect of Mst1 knockdown on hepatocyte mitochondrial stress

To explain the protective effects exerted by Parkin-related mitophagy on PA-treated hepatocytes, mitochondrial function and cell apoptosis were detected. Firstly, mitochondrial potential, assessed by JC-1 staining, was significantly reduced by PA treatment (Fig. 6A-B). Interestingly, Mst1 knockdown stabilized mitochondrial potential; this effect was abolished by Parkin siRNA transfection (Fig. 6A-B). Besides, mitochondrial ROS production, assessed by flow cytometery, was obviously increased in response to PA stress (Fig. 6C). However, Mst1 knockdown attenuated mROS overloading via reversing Parkin-related mitophagy. Besides, the opening rate of mPTP was drastically increased in PA-treated cells and was reduced to near-normal levels with Mst1 knockdown in a manner dependent on Parkin-related mitophagy (Fig. 6D).

The cyt-c liberation from mitochondria into cytoplasm/nucleus is the molecular feature of mitochondrial apoptosis. Interestingly, PA-mediated cyt-c translocation from mitochondria into cytoplasm could be inhibited by Mst1 knockdown in a manner dependent on Parkin-related mitophagy (Fig. 6E-F). To the end, hepatocyte mitochondrial apoptosis, as assessed by caspase-9 activity detection, was markedly increased in response to PA challenge (Fig. 6G). However, loss of Mst1 prevented PA-induced caspase-9 activation, and this effect was invalidated by Parkin siRNA transfection (Fig. 6G). Taken together, the above data illustrated that Parkin-related mitophagy was required for the protective effects of Mst1 knockdown on hepatic mitochondrial homeostasis under high-fat stress.

3.7. Mst1 modulates Parkin via activating AMPK pathway

Previous study has reported that AMPK pathway is involved in mitophagy management [39,40]. In the present study, we questioned whether AMPK was involved in Mst1-modified Parkin mitophagy. Western blotting analysis demonstrated that the expression of phosphorylated AMPK was drastically donwregulated in PA-treated cells (Fig. 7A-C), and this effect would be abolished by Mst1 knockdown. Subsequently, an antagonst of the AMPK pathway (Compound C, CC) was added into the medium of Mst1-deleted cells to prevent AMPK activation, and then, Parkin expression was monitored. As shown in Fig. 7A-C, PA-mediated Parkin downregulation could be abolished by Mst1 knockdown, and this effect was nullified by CC. This finding was further verified via immunofluorescence. As shown in Fig. 7D-F, PA treatment significantly suppressed the fluorescence intensities of p-AMPK and Parkin in hepatocytes; this alterations could be abrogated by Mst1 knockdown. Interestingly, blockade of AMPK pathway prevented

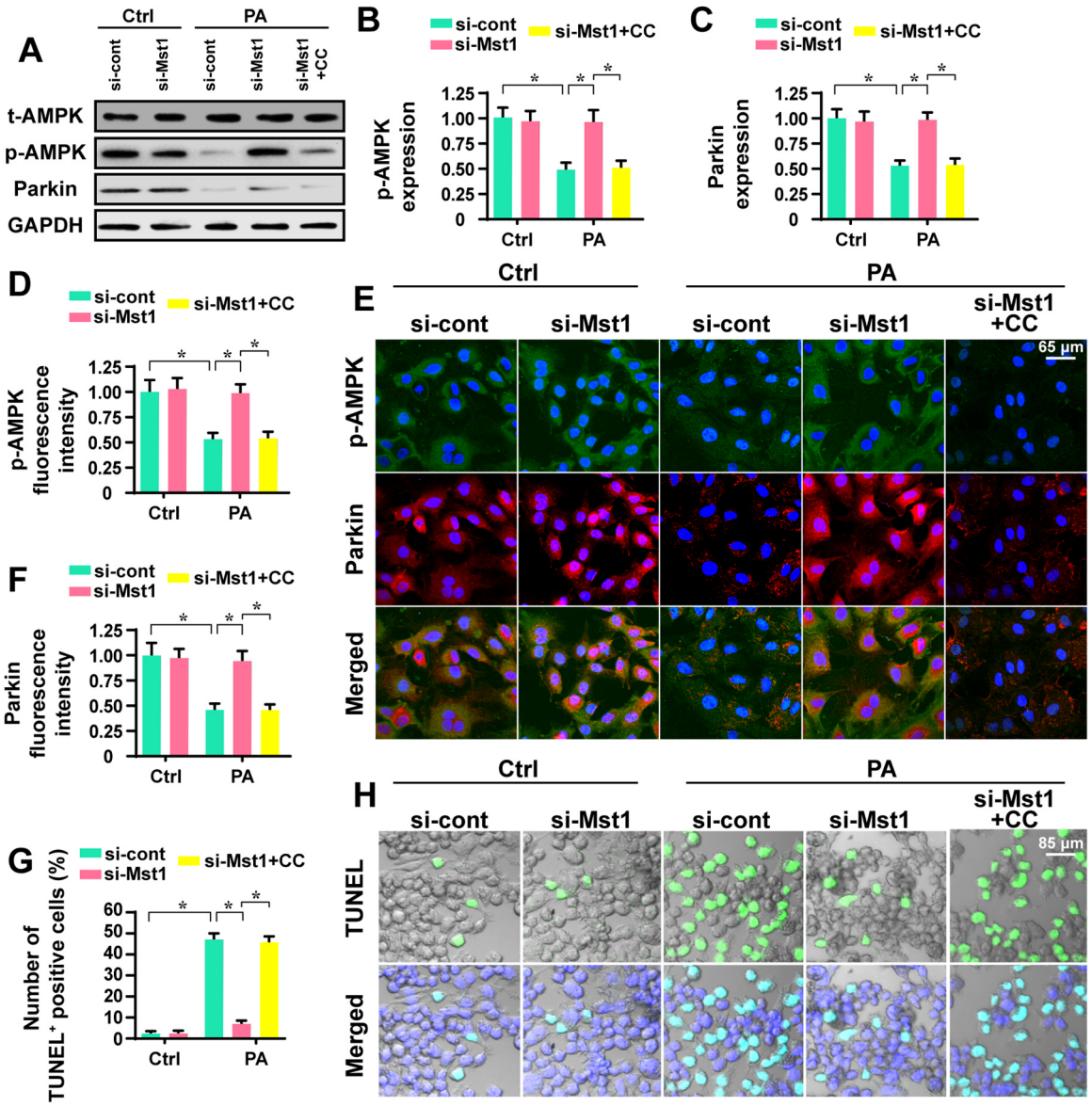

Fig. 7. Mst1 regulates Mst1 via the AMPK pathway. A-C. *In vitro*, primary hepatocytes were treated with PA and then, proteins were isolated from cells. Western blotting was used to analyse the expression of AMPK and Parkin. Compound C (CC), an inhibitor of AMPK, was added into the medium of cells to inhibit AMPK activation. D-F. Immunofluorescence assay for Parkin and p-AMPK. G-H. TUNEL assay was used to observe the cell apoptosis. The number of TUNEL-positive cell was recorded in response to Mst1 knockdown and CC incubation. Experiments were repeated three times and data are shown as the means ± SEM. n = 6 mice per group. $^{*}P < 0.05$.

Parkin upregulation in Mst1-deleted cells. These information indicated that Mst1 knockdown reversed Parkin expression via activating AMPK pathway.

With respect to hepatocyte apoptosis, TUNEL assay was used. As shown in Fig. 7G-H, Mst1 knockdown reduced the PA-mediated hepatocyte apoptosis, and this effect was nullified by CC, suggesting that AMPK pathway was also implicated in Mst1-modified hepatocyte viability under PA stress.

4. Discussion

Many researchers have attempted to demonstrate the protective role played by mitophagy in attenuating fatty liver disease [9,41]. However, there have been no studies investigating the upstream regulatory mechanisms for mitophagy management in the progression of NAFLD. In the present study, our data illustrated that (1) HFD-mediated fatty liver disease was attributable to Mst1 upregulation, (2) increased Mst1 promoted liver vacuolation, steatosis, fibrosis, oxidative stress and the inflammation injury, (3) genetic ablation of Mst1 attenuated the HFD-mediated hepatic injury via sustaining hepatocyte viability, (4) mechanistically, Mst1 knockdown protected hepatocyte mitochondrial function and blocked mitochondria apoptosis in a manner dependent on Parkin-related mitophagy, (6) knockdown of Parkin abolished the protective effects exerted by Mst1 knockdown on HFD-treated livers, (7) ultimately, we further demonstrated that Mst1 modulated Parkin-related mitophagy via the AMPK pathway. To the best of our knowledge, this is the first study to describe the comprehensive role of Mst1 in HFD-mediated hepatic injury via *in vivo* and *in vitro* studies. Our findings provide a potential target to prevent liver dysfunction in patients with obesity-related liver disease. However, more clinical evidence is required in the future to support this concept.

NAFLD, which is the most common chronic liver disease in the Western world, represents an aggressive disease entity that is visible as hepatocyte ballooning, an inflammatory infiltrate, collagen deposition and hepatocyte death [42]. Multiple cell-intrinsic mechanisms have been suggested to trigger cell death and the progression to NAFLD

[43,44]. Recently, it has been recognized that impaired hepatic mitochondrial function plays a key role in the progression of hepatocyte death [45]. Chronic lipid accumulation shifts the mitochondrial metabolism to beta-oxidation, and contributes to the overproduction of ROS and mitochondrial metabolism dysfunction [46]. In our study, we found that HFD treatment indeed induced the mitochondrial dysfunction, as revealed by oxidative stress, cyt-c release, ATP metabolism disorder, and caspase-9-involved mitochondrial apoptosis pathway activation. This information reconfirm that mitochondria protection is the therapeutic target that retards the progression of NAFLD.

In response to mitochondrial damage, mitochondria could employ mitophagy to remove the injured mitochondria [47]. However, the activity of mitophagy was significantly repressed by high-fat stress via Mst1. These conclusions identify Mst1 as the upstream inhibitor for mitophagy. Our studies were in accordance with several previous studies. In cardiac ischemia-reperfusion, increased Mst1 suppresses FUNDC1-related mitophagy and then exacerbates mitochondrial damage and cardiomyocyte death [13]. Besides, in colorectal cancer, increased Mst1 also inhibits mitophagy activity in a manner dependent on JNK/p53/Bnip3 pathways [16]. In endometriosis, activated Mst1 promotes endometrial stromal cells apoptosis via repressing Parkin-related mitophagy [15]. Based on these findings, the inhibition of Mst1 activity is of utmost importance when designing liver-protective therapies to attenuate fatty liver disease via reversing mitophagy.

At the molecular levels, mitophagy is primarily regulated by several mitophagic receptors. For example, FUNDC1, the mitochondrial outer membrane proteins, has been acknowledged as the guard of liver function in the setting of hepatocellular carcinoma [6]. In addition, Bnip3, another mitochondrial receptor, exerts beneficial effects on HFD-treated liver tissues [12]. However, little study is available to establish the role of Parkin in fatty liver disease. This study demonstrated that Parkin was unfortunately downregulated in HFD-treated liver tissues. Genetic ablation of Mst1 reversed Parkin expression and this effect was achieved via activating the AMPK pathway. Blockade of AMPK pathway abolished the promotive effects of Mst1 knockdown on Parkin upregulation. Notably, more robust data concerning the relationship of the AMPK pathway and mitophagy have been provided by genetic loss- and gain-of- function studies [48–50]. However, whether Mst1 could modulate mitophagy via other receptors in a manner dependent on the AMPK pathway is far from clear.

Altogether, our results implicate Mst1 upregulation as a critical step in exacerbating HFD-mediated hepatic injury. Increased Mst1 blocks the AMPK pathway and thus diminishes Parkin expression, repressing mitophagy and consequently activating mitochondrial apoptosis in HFD-treated livers. Thus, our findings reveal a novel molecular mechanism for the development of fatty liver disease and suggest the regulatory importance of Mst1 and Parkin-mediated mitophagy in preserving hepatocyte mitochondrial homeostasis.

Acknowledgments

Not applicable.

Funding

This study was supported by the Scientific and Technological Innovation and Action Project of Shanghai Science and Technology Commission (Grant No. 15411950401) Shanghai Pudong Commission of Health and Family Planning (PWRd2016-12) and Talents Training Program of Seventh People's Hospital of Shanghai University of TCM (BDX2016-01).

Conflict of interest statement

The authors have declared that they have no conflicts of interest.

References

[1] H. Zhou, W. Du, Y. Li, C. Shi, N. Hu, S. Ma, W. Wang, J. Ren, Effects of melatonin on fatty liver disease: the role of NR4A1/DNA-PKcs/p53 pathway, mitochondrial fission, and mitophagy, J. Pineal Res. 64 (1) (2018).
[2] R. Li, T. Xin, D. Li, C. Wang, H. Zhu, H. Zhou, Therapeutic effect of Sirtuin 3 on ameliorating nonalcoholic fatty liver disease: the role of the ERK-CREB pathway and Bnip3-mediated mitophagy, Redox Biol. 18 (2018) 229–243.
[3] I.C.M. Simoes, A. Fontes, P. Pinton, H. Zischka, M.R. Wieckowski, Mitochondria in non-alcoholic fatty liver disease, Int. J. Biochem. Cell Biol. 95 (2018) 93–99.
[4] H. Zhou, P. Zhu, J. Wang, H. Zhu, J. Ren, Y. Chen, Pathogenesis of cardiac ischemia reperfusion injury is associated with CK2alpha-disturbed mitochondrial homeostasis via suppression of FUNDC1-related mitophagy, Cell Death Differ. 25 (6) (2018) 1080–1093.
[5] A. Blazquez-Castro, Direct (1)O2 optical excitation: a tool for redox biology, Redox Biol. 13 (2017) 39–59.
[6] W. Li, Y. Li, S. Siraj, H. Jin, Y. Fan, X. Yang, X. Huang, X. Wang, J. Wang, L. Liu, L. Du, Q. Chen, FUNDC1-mediated mitophagy suppresses hepatocarcinogenesis by inhibition of inflammasome activation, Hepatology (2018).
[7] H. Zhou, J. Wang, P. Zhu, H. Zhu, S. Toan, S. Hu, J. Ren, Y. Chen, NR4A1 aggravates the cardiac microvascular ischemia reperfusion injury through suppressing FUNDC1-mediated mitophagy and promoting Mff-required mitochondrial fission by CK2alpha, Basic Res. Cardiol. 113 (4) (2018) 23.
[8] R.H. Bhogal, C.J. Weston, S. Velduis, H.G.D. Leuvenink, G.M. Reynolds, S. Davies, L.N. Thin, M. Alfaifi, E. Shepard, Y. Boteon, L. Wallace, Y. Oo, D.H. Adams, D.F. Mirza, H. Mergental, G. Muirhead, B.F. Stephenson, S.C. Afford, The ROS-mitophagy signalling pathway regulates liver endothelial cell survival during ischaemia-reperfusion injury, Liver Transpl. (2018).
[9] T. Yamada, D. Murata, Y. Adachi, K. Itoh, S. Kameoka, A. Igarashi, T. Kato, Y. Araki, R.L. Huganir, T.M. Dawson, T. Yanagawa, K. Okamoto, M. Iijima, H. Sesaki, Mitochondrial stasis reveals p62-mediated ubiquitination in parkin-independent mitophagy and mitigates nonalcoholic fatty liver disease, Cell Metab. (2018).
[10] G. Loforese, T. Malinka, A. Keogh, F. Baier, C. Simillion, M. Montani, T.D. Halazonetis, D. Candinas, D. Stroka, Impaired liver regeneration in aged mice can be rescued by silencing Hippo core kinases MST1 and MST2, EMBO Mol. Med. 9 (1) (2017) 46–60.
[11] C. Geng, Y. Zhang, Y. Gao, W. Tao, H. Zhang, X. Liu, F. Fang, Y. Chang, Mst1 regulates hepatic lipid metabolism by inhibiting Sirt1 ubiquitination in mice, Biochem. Biophys. Res. Commun. 471 (4) (2016) 444–449.
[12] S.H. Jeong, H.B. Kim, M.C. Kim, J.M. Lee, J.H. Lee, J.H. Kim, J.W. Kim, W.Y. Park, S.Y. Kim, J.B. Kim, H. Kim, J.M. Kim, H.S. Choi, D.S. Lim, Hippo-mediated suppression of IRS2/AKT signaling prevents hepatic steatosis and liver cancer, J. Clin. Investig. 128 (3) (2018) 1010–1025.
[13] W. Yu, M. Xu, T. Zhang, Q. Zhang, C. Zou, Mst1 promotes cardiac ischemia-reperfusion injury by inhibiting the ERK-CREB pathway and repressing FUNDC1-mediated mitophagy, J. Physiol. Sci. (2018).
[14] H. Zhou, P. Zhu, J. Guo, N. Hu, S. Wang, D. Li, S. Hu, J. Ren, F. Cao, Y. Chen, Ripk3 induces mitochondrial apoptosis via inhibition of FUNDC1 mitophagy in cardiac IR injury, Redox Biol. 13 (2017) 498–507.
[15] Q. Zhao, M. Ye, W. Yang, M. Wang, M. Li, C. Gu, L. Zhao, Z. Zhang, W. Han, W. Fan, Y. Meng, Effect of Mst1 on endometriosis apoptosis and migration: role of Drp1-related mitochondrial fission and parkin-required mitophagy, Cell Physiol. Biochem. 45 (3) (2018) 1172–1190.
[16] Q. Li, F. Qi, X. Meng, C. Zhu, Y. Gao, Mst1 regulates colorectal cancer stress response via inhibiting Bnip3-related mitophagy by activation of JNK/p53 pathway, Cell Biol. Toxicol. (2017).
[17] M. Zhang, J. Lin, S. Wang, Z. Cheng, J. Hu, T. Wang, W. Man, T. Yin, W. Guo, E. Gao, R.J. Reiter, H. Wang, D. Sun, Melatonin protects against diabetic cardiomyopathy through Mst1/Sirt3 signaling, J. Pineal Res. 63 (2) (2017).
[18] A. Bikfalvi, History and conceptual developments in vascular biology and angiogenesis research: a personal view, Angiogenesis 20 (4) (2017) 463–478.
[19] N.J.R. Blackburn, B. Vulesevic, B. Mcneill, C.E. Cimenci, A. Ahmadi, M. Gonzalez-Gomez, A. Ostojic, Z. Zhong, M. Brownlee, P.J. Beisswenger, R.W. Milne, E.J. Suuronen, Methylglyoxal-derived advanced glycation end products contribute to negative cardiac remodeling and dysfunction post-myocardial infarction, Basic Res. Cardiol. 112 (5) (2017) 57.
[20] R.G. Abeysuriya, S.W. Lockley, P.A. Robinson, S. Postnova, A unified model of melatonin, 6-sulfatoxymelatonin, and sleep dynamics, J. Pineal Res. 64 (4) (2018) e12474.
[21] N. Alvarez-Sanchez, I. Cruz-Chamorro, M. Diaz-Sanchez, H. Sarmiento-Soto, P. Medrano-Campillo, A. Martinez-Lopez, P.J. Lardone, J.M. Guerrero, A. Carrillo-Vico, Melatonin reduces inflammatory response in peripheral T helper lymphocytes from relapsing-remitting multiple sclerosis patients, J. Pineal Res. 63 (4) (2017).
[22] X. Ba, I. Boldogh, 8-Oxoguanine DNA glycosylase 1: beyond repair of the oxidatively modified base lesions, Redox Biol. 14 (2018) 669–678.
[23] H. Zhou, J. Wang, P. Zhu, S. Hu, J. Ren, Ripk3 regulates cardiac microvascular reperfusion injury: the role of IP3R-dependent calcium overload, XO-mediated oxidative stress and F-action/filopodia-based cellular migration, Cell Signal. 45 (2018) 12–22.
[24] Q. Jin, R. Li, N. Hu, T. Xin, P. Zhu, S. Hu, S. Ma, H. Zhu, J. Ren, H. Zhou, DUSP1 alleviates cardiac ischemia/reperfusion injury by suppressing the Mff-required mitochondrial fission and Bnip3-related mitophagy via the JNK pathways, Redox Biol. 14 (2018) 576–587.
[25] H. Hong, T. Tao, S. Chen, C. Liang, Y. Qiu, Y. Zhou, R. Zhang, MicroRNA-143 promotes cardiac ischemia-mediated mitochondrial impairment by the inhibition of

protein kinase Cepsilon, Basic Res. Cardiol. 112 (6) (2017) 60.
[26] L.Y. Chen, T.Y. Renn, W.C. Liao, F.D. Mai, Y.J. Ho, G. Hsiao, A.W. Lee, H.M. Chang, Melatonin successfully rescues hippocampal bioenergetics and improves cognitive function following drug intoxication by promoting Nrf2-ARE signaling activity, J. Pineal Res. 63 (2) (2017).
[27] H. Zhou, S. Hu, Q. Jin, C. Shi, Y. Zhang, P. Zhu, Q. Ma, F. Tian, Y. Chen, Mff-dependent mitochondrial fission contributes to the pathogenesis of cardiac microvasculature ischemia/reperfusion injury via induction of mROS-mediated cardiolipin oxidation and HK2/VDAC1 disassociation-involved mPTP opening, J. Am. Heart Assoc. 6 (3) (2017).
[28] D. Brasacchio, A.E. Alsop, T. Noori, M. Lufti, S. Iyer, K.J. Simpson, P.I. Bird, R.M. Kluck, R.W. Johnstone, J.A. Trapani, Epigenetic control of mitochondrial cell death through PACS1-mediated regulation of BAX/BAK oligomerization, Cell Death Differ. 24 (6) (2017) 961–970.
[29] H. Zhou, Y. Yue, J. Wang, Q. Ma, Y. Chen, Melatonin therapy for diabetic cardiomyopathy: a mechanism involving Syk-mitochondrial complex I-SERCA pathway, Cell Signal. 47 (2018) 88–100.
[30] A.M. Kiel, A.G. Goodwill, J.N. Noblet, A.L. Barnard, D.J. Sassoon, J.D. Tune, Regulation of myocardial oxygen delivery in response to graded reductions in hematocrit: role of K(+) channels, Basic Res. Cardiol. 112 (6) (2017) 65.
[31] C. Cheignon, M. Tomas, D. Bonnefont-Rousselot, P. Faller, C. Hureau, F. Collin, Oxidative stress and the amyloid beta peptide in Alzheimer's disease, Redox Biol. 14 (2018) 450–464.
[32] C. Shi, Y. Cai, Y. Li, Y. Li, N. Hu, S. Ma, S. Hu, P. Zhu, W. Wang, H. Zhou, Yap promotes hepatocellular carcinoma metastasis and mobilization via governing cofilin/F-actin/lamellipodium axis by regulation of JNK/Bnip3/SERCA/CaMKII pathways, Redox Biol. 14 (2018) 59–71.
[33] S.I. Choi, E. Lee, B. Akuzum, J.B. Jeong, Y.S. Maeng, T.I. Kim, E.K. Kim, Melatonin reduces endoplasmic reticulum stress and corneal dystrophy-associated TGFBIp through activation of endoplasmic reticulum-associated protein degradation, J. Pineal Res. 63 (3) (2017).
[34] P. Zhu, S. Hu, Q. Jin, D. Li, F. Tian, S. Toan, Y. Li, H. Zhou, Y. Chen, Ripk3 promotes ER stress-induced necroptosis in cardiac IR injury: a mechanism involving calcium overload/XO/ROS/mPTP pathway, Redox Biol. 16 (2018) 157–168.
[35] M. Morell, J.I. Burgos, L.A. Gonano, M. Vila Petroff, AMPK-dependent nitric oxide release provides contractile support during hyperosmotic stress, Basic Res. Cardiol. 113 (1) (2017) 7.
[36] T. Lagerweij, S.A. Dusoswa, A. Negrean, E.M.L. Hendrikx, H.E. De Vries, J. Kole, J.J. Garcia-Vallejo, H.D. Mansvelder, W.P. Vandertop, D.P. Noske, B.A. Tannous, R.J.P. Musters, Y. Van Kooyk, P. Wesseling, X.W. Zhao, T. Wurdinger, Optical clearing and fluorescence deep-tissue imaging for 3D quantitative analysis of the brain tumor microenvironment, Angiogenesis 20 (4) (2017) 533–546.
[37] E. Villa, S. Marchetti, J.E. Ricci, No Parkin Zone: mitophagy without Parkin, Trends Cell Biol. (2018).
[38] W. Zhang, H. Ren, C. Xu, C. Zhu, H. Wu, D. Liu, J. Wang, L. Liu, W. Li, Q. Ma, L. Du, M. Zheng, C. Zhang, J. Liu, Q. Chen, Hypoxic mitophagy regulates mitochondrial quality and platelet activation and determines severity of I/R heart injury, Elife 5 (2016).
[39] A. Onnis, V. Cianfanelli, C. Cassioli, D. Samardzic, P.G. Pelicci, F. Cecconi, C.T. Baldari, The pro-oxidant adaptor p66SHC promotes B cell mitophagy by disrupting mitochondrial integrity and recruiting LC3-II, Autophagy (2018).
[40] C. Liu, J. Wang, Y. Yang, X. Liu, Y. Zhu, J. Zou, S. Peng, T.H. Le, Y. Chen, S. Zhao, B. He, Q. Mi, X. Zhang, Q. Du, Ginsenoside Rd ameliorates colitis by inducing p62-driven mitophagy-mediated NLRP3 inflammasome inactivation in mice, Biochem. Pharmacol. 155 (2018) 366–379.
[41] A. Von Schulze, C.S. Mccoin, C. Onyekere, J. Allen, P. Geiger, G.W. Dorn 2nd, E.M. Morris, J.P. Thyfault, Hepatic mitochondrial adaptations to physical activity: impact of sexual dimorphism, PGC1alpha, and BNIP3 mediated mitophagy, J. Physiol. (2018).
[42] J. Liu, S. Jiang, Y. Zhao, Q. Sun, J. Zhang, D. Shen, J. Wu, N. Shen, X. Fu, X. Sun, D. Yu, J. Chen, J. He, T. Shi, Y. Ding, L. Fang, B. Xue, C. Li, Geranylgeranyl diphosphate synthase (GGPPS) regulates NAFLD/fibrosis progression by determining hepatic glucose/fatty acid preference under high-fat-diet conditions, J. Pathol. (2018).
[43] Y. Saito, H. Hikita, Y. Nozaki, Y. Kai, Y. Makino, T. Nakabori, S. Tanaka, R. Yamada, M. Shigekawa, T. Kodama, R. Sakamori, T. Tatsumi, T. Takehara, DNase II activated by the mitochondrial apoptotic pathway regulates RIP1-dependent non-apoptotic hepatocyte death via the TLR9/IFN-beta signaling pathway, Cell Death Differ. (2018).
[44] M.G. Zhao, X.P. Sheng, Y.P. Huang, Y.T. Wang, C.H. Jiang, J. Zhang, Z.Q. Yin, Triterpenic acids-enriched fraction from Cyclocarya paliurus attenuates non-alcoholic fatty liver disease via improving oxidative stress and mitochondrial dysfunction, Biomed. Pharmacother. 104 (2018) 229–239.
[45] E.M. Sullivan, E.R. Pennington, W.D. Green, M.A. Beck, D.A. Brown, S.R. Shaikh, Mechanisms by which dietary fatty acids regulate mitochondrial structure-function in health and disease, Adv. Nutr. 9 (3) (2018) 247–262.
[46] J. Le, W. Jia, Y. Sun, Sennoside A protects mitochondrial structure and function to improve high-fat diet-induced hepatic steatosis by targeting VDAC1, Biochem. Biophys. Res. Commun. 500 (2) (2018) 484–489.
[47] P. Liu, H. Lin, Y. Xu, F. Zhou, J. Wang, J. Liu, X. Zhu, X. Guo, Y. Tang, P. Yao, Frataxin-mediated PINK1-parkin-dependent mitophagy in hepatic steatosis: the protective effects of quercetin, Mol. Nutr. Food Res. (2018) e1800164.
[48] K.A. Boyle, J. Van Wickle, R.B. Hill, A. Marchese, B. Kalyanaraman, M.B. Dwinell, Mitochondria-targeted drugs stimulate mitophagy and abrogate colon cancer cell proliferation, J. Biol. Chem. (2018).
[49] W. Tian, W. Li, Y. Chen, Z. Yan, X. Huang, H. Zhuang, W. Zhong, Y. Chen, W. Wu, C. Lin, H. Chen, X. Hou, L. Zhang, S. Sui, B. Zhao, Z. Hu, L. Li, D. Feng, Phosphorylation of ULK1 by AMPK regulates translocation of ULK1 to mitochondria and mitophagy, FEBS Lett. 589 (15) (2015) 1847–1854.
[50] B. Wang, J. Nie, L. Wu, Y. Hu, Z. Wen, L. Dong, M.H. Zou, C. Chen, D.W. Wang, AMPKalpha2 protects against the development of heart failure by enhancing mitophagy via PINK1 phosphorylation, Circ. Res. 122 (5) (2018) 712–729.